Absolute frequency measurement of a Yb optical clock at the limit of the Cs fountain

Metrologia

Absolute frequency measurement of a Yb optical clock at the limit of the Cs fountain

OPEN ACCESS
IOP Publishing | Bureau International des Poids et Mesures Metrologia
Metrologia **60** (2023) 035002 (7pp) https://doi.org/10.1088/1681-7575/accbc5

Absolute frequency measurement of a Yb optical clock at the limit of the Cs fountain

Irene Goti[1,2], Stefano Condio[1,2], Cecilia Clivati[1], Matias Risaro[1], Michele Gozzelino[1], Giovanni A Costanzo[1,2], Filippo Levi[1], Davide Calonico[1] and Marco Pizzocaro[1,*]

[1] Istituto Nazionale di Ricerca Metrologica (INRiM), Strada delle Cacce 91, 10135 Torino, Italy
[2] Dipartimento di Elettronica e Telecomunicazioni, Politecnico di Torino, Corso duca degli Abruzzi 24, 10129 Torino, Italy

E-mail: m.pizzocaro@inrim.it

Received 21 December 2022, revised 6 March 2023
Accepted for publication 11 April 2023
Published 3 May 2023

Abstract

We present the new absolute frequency measurement of ytterbium (^{171}Yb) obtained at INRiM with the optical lattice clock IT-Yb1 against the cryogenic caesium (^{133}Cs) fountain IT-CsF2, evaluated through a measurement campaign that lasted 14 months. Measurements are performed by either using a hydrogen maser as a transfer oscillator or by synthesizing a low-noise microwave for Cs interrogation using an optical frequency comb. The frequency of the ^{171}Yb unperturbed clock transition $^1S_0 \rightarrow {}^3P_0$ results to be 518 295 836 590 863.44(14) Hz, with a total fractional uncertainty of 2.7×10^{-16} that is limited by the uncertainty of IT-CsF2. Our measurement is in agreement with the Yb frequency recommended by the Consultative Committee for Time and Frequency. This result confirms the reliability of Yb as a secondary representation of the second and is relevant to the process of redefining the second in the International System of Units on an optical transition.

Keywords: frequency metrology, optical lattice clock, Cs fountain, SI second

(Some figures may appear in colour only in the online journal)

1. Introduction

The definition of the International System of Unit (SI) second is currently realized through a Cs frequency transition in the microwave regime [1–11]. Nevertheless, in recent years it has been widely demonstrated that optical clocks represent a better frequency standard [12–15], both in terms of fractional frequency instability and estimated systematic uncertainty. Specific optical transitions are currently indicated by the Consultative Committee for Time and Frequency (CCTF) as secondary representations of the SI second, and recent progress in the field of optical clocks paves the way to a redefinition of the SI second [16–18]. In 2022, the CCTF published a roadmap stating relevant milestones to be achieved to proceed to a redefinition of the SI second, among which emerge multiple and independent measurements of optical clocks relative to independent Cs primary clocks. One of the secondary representations of the second recommended by the CCTF is the transition $^1S_0 \rightarrow {}^3P_0$ of ^{171}Yb. Absolute frequency measurements of this clock transition have been realized by several metrological institutes worldwide [14, 19–27]. At INRiM we measured the absolute frequency of the ^{171}Yb clock (IT-Yb1) relative to our local cryogenic Cs fountain (IT-CsF2) [28] and via International Atomic Time (TAI) [29]. Moreover, we measured the frequency ratio between ^{171}Yb

* Author to whom any correspondence should be addressed.

and ^{87}Sr clock with a transportable optical Sr clock developed at PTB [30], and via very long baseline interferometry in collaboration with NICT, INAF, and the International Bureau of Weights and Measures (BIPM) [31]. Recently we used the new fiber link between INRiM and SYRTE to measure the Yb clock frequency against the french Cs–Rb fountain [19].

In this article, we report the improvements of our optical lattice clock IT-Yb1 and the results obtained from a new measurement of the Yb absolute frequency against IT-CsF2 over a period of 14 months. The frequency measurement is performed with two different techniques: with the first method, the hydrogen maser is used as a transfer oscillator between the optical clock and the fountain, while with the second method the microwave interrogating the fountain is directly obtained by photonic synthesis on a frequency comb, using the Yb clock laser as a local oscillator.

This paper is organized as follows: in section 2 we describe the main components of our experimental setup, i.e. the Yb clock, the Cs fountain and the two measurement techniques. In section 3 we report the results obtained in terms of Yb absolute frequency. Finally, section 4 presents the conclusions of our work.

2. Experimental setup

2.1. IT-Yb1 and IT-CsF2

IT-Yb1 is the optical lattice clock based on ^{171}Yb atoms developed at INRiM. The uncertainty budget of IT-Yb1 during this measurement campaign is reported in table 1 and the total relative uncertainty is 1.9×10^{-17}. The typical instability of IT-Yb1 is $2 \times 10^{-15}/\sqrt{\tau/\mathrm{s}}$. IT-Yb1 is among the optical clocks that regularly submit data to the BIPM for the calibration of TAI [25, 27, 29, 32, 33].

IT-Yb1 and its details have been described in previous work [28, 29]. An ultrastable laser at 1156 nm is frequency doubled to generate the 578 nm light that is kept resonant with the ^{171}Yb clock transition $^1\mathrm{S}_0 \rightarrow {}^3\mathrm{P}_0$. A new ultrastable cavity directly stabilizes the 1156 nm radiation instead of its second harmonic at 578 nm. It is a horizontal 10 cm-long cavity, made in ultra-low-expansion glass and fused silica mirror, characterized by a flicker floor of $\sim 1 \times 10^{-15}$. Compared to previous publications we improved the evaluation of the lattice shift and the static stark shift. In particular, we changed the optical setup from a horizontal to a vertical optical lattice with the advantage of having the strong axis of the trap contrasting the gravity. In this way, we managed to reduce the minimum trapping depth to 75 E_r, where $E_\mathrm{r} \simeq h \times 2$ kHz is the recoil energy for Yb and h is the Plank constant. We also decreased the depth of our working point from 200 E_r [28] to 100 E_r, with consequent advantages in terms of uncertainty budget. The working point of the lattice frequency is chosen at $\nu_\mathrm{lattice} = 394\,798\,267$ MHz, and it is continuously measured by an optical comb. Moreover, atoms are loaded into the lattice directly at the working depth U, making the atomic temperature of the trapped atoms linear as a function of the lattice depth. It is then possible to apply the approach described in [34, 35] and calculate the relative lattice shift by following the model: $\frac{\delta\nu}{\nu} = -\alpha U - \beta U^2$, where α and β are two parameters that have to be measured in the specific experimental conditions. We estimate a model uncertainty of 1×10^{-17} [34] resulting from deviation from linearity between the atomic temperature and the lattice depth.

Table 1. Uncertainty budget of IT-Yb1. Other shifts are AOM switching, fiber links, and line pulling.

Effect	Rel. Shift/10^{-17}	Rel. Unc./10^{-17}
Density shift	−0.5	0.2
Lattice shift	0.8	1.2
Zeeman shift	−3.12	0.02
Blackbody radiation shift (room)	−234.9	1.2
Blackbody radiation shift (oven)	−1.3	0.6
Static Stark shift	−1.7	0.2
Probe light shift	0.04	0.03
Background gas shift	−0.5	0.2
Servo error	0.0	0.3
Other shifts	0.0	0.1
Grav. redshift	2599.5	0.3
Total	2358.3	1.9

We note that, since the density shift is smaller for lower lattice depth [36], at the new working point of 100 E_r the density shift is reduced by a factor of 10 if compared to previous work [29]. Furthermore, the atomic tunneling between adjacent lattice sites is suppressed in a vertical lattice [14, 37], making this source of uncertainty negligible.

Eight electrodes are placed on the vertical windows, four on the top window and four on the bottom, to evaluate the static stark shift. By applying voltages of up to ±150 V independently to each electrode, it is possible to measure its contribution along the three spatial directions [38, 39]. With this new setup, we detect a stray electric field of about 1 V cm^{-1} to 2 V cm^{-1} on the horizontal plane, which is found to change slightly from day to day and with no significant trend during the campaign. One possible explanation is photoionization from the 399 nm laser beams on the window coating [40–42]. However, the low-laser intensity and the direction of the electric field suggest that the oven used to generate the Yb atomic beam emits ionized particles that accumulate on the windows and reach a dynamic equilibrium. We manage to compensate for the stray electric field by using the same electrodes. The electric field in the three directions is measured typically three times per week. As each measurement is independent and limited by measurement instability, we allow the resulting shift to be averaged over the campaign. The resulting shift for the period considered in this work is reported in table 1.

IT-CsF2 is a cryogenic Cs fountain [10] and since 2013 it operates as a primary frequency standard contributing to the realization of UTC(IT) and TAI, with over 50 TAI calibration campaigns performed and published on the BIPM circular T. The uncertainty budget of IT-CsF2 is reported in table 2 and the total relative uncertainty is 2.3×10^{-16}.

The density shift is evaluated by alternating clock measurements with two different atom numbers and

Table 2. Uncertainty budget of IT-CsF2.

Effect	Rel. Shift/10^{-16}	Rel. Unc./10^{-16}
Zeeman shift	1080.3	0.8
Blackbody radiation	−1.45	0.12
Gravitational redshift	260.4	0.1
Microwave leakage	−1.2	1.4
DCP (distributed cavity phase)	—	0.2
Second order cavity pulling	—	0.3
Background gas	—	0.5
Density shift	−19.8	1.6
Total	1318.2	2.3

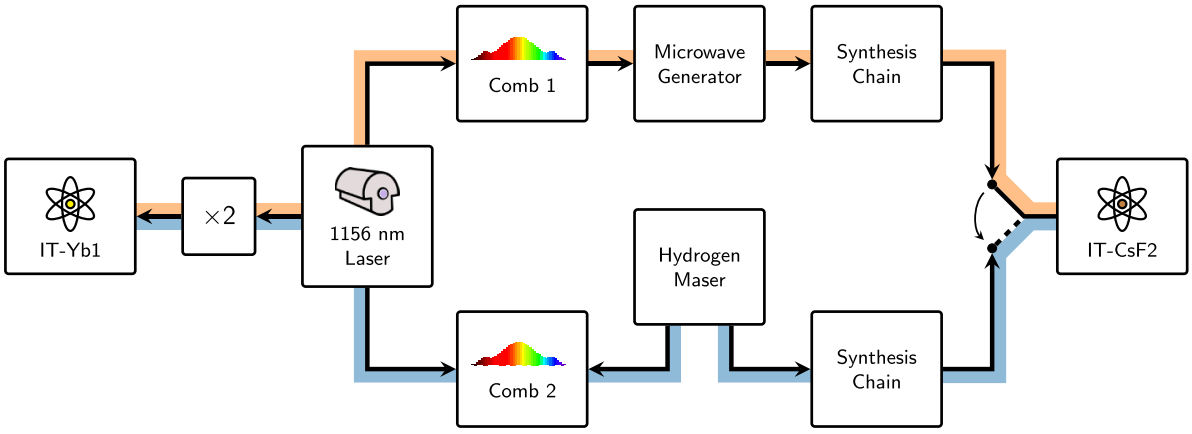

Figure 1. Experimental setup scheme of IT-Yb1 absolute frequency measurement against IT-CsF2 clock. In blue is represented the path of the H-maser chain, which is our usual measurement chain. In orange instead is shown the Optical Microwave chain: a new measurement technique we tested in this campaign.

extrapolating to zero-density. Indeed, the knowledge of the collisional-shift parameter for performing the extrapolation progressively improves with time, as its computation takes advantage of using historical and newly accumulated data, until some parameter characterizing the shift does change, requiring a new measurement run to re-calibrate the density-shift extrapolation.

In its usual configuration, the local oscillator for this clock is a BVA quartz phase-locked to an H-maser and upconverted to 9.2 GHz using cascaded multiplication stages and a dielectric resonator oscillator [10]. This signal is tuned to the atomic resonance using a direct digital synthesizer (DDS) at about 7.4 MHz, adjusted at each interrogation cycle. The typical short-term stability of IT-CsF2 results from a combination of the Dick effect due to the BVA quartz noise and the atomic background noise due to hot Cs atoms. It ranges between $2.4 \times 10^{-13}/\sqrt{\tau/\mathrm{s}}$ in high density regime and $2.8 \times 10^{-13}/\sqrt{\tau/\mathrm{s}}$ at low density.

2.2. The measurement chain

Figure 1 shows the block diagram of the two measurement chains used to compare IT-Yb1 and IT-CsF2. The usual measurement scheme is represented in the lower branch (blue path, hereafter referenced to as 'H-maser chain'). The radiation at 1156 nm, frequency-stabilized to the ultrastable cavity, is doubled to 578 nm for interrogating the ^{171}Yb clock transition. Part of it is also beaten to a fiber frequency comb stabilized to the same BVA quartz/H-maser system that serves as a local oscillator for IT-CsF2. The IT-Yb1/IT-CsF2 ratio can thus be computed using the comb and H-maser as transfer oscillators. Some of the measurements are instead collected using the measurement chain shown in figure 1 with the orange path (hereafter referred to as 'Optical Microwave chain'). In this configuration, the frequency comb is referenced to the ultrastable 1156 nm radiation and operates as a low-noise microwave generator to synthesize a signal resonant with the Cs clock transition [43, 44]. The coherent spectral transfer between optical and microwave frequencies is obtained by tightly phase-locking the comb to the optical reference (bandwidth ≈300 kHz), following a scheme similar to the one described in [43]. The comb pulse train is collected by a fast photodiode, where the 40th harmonic of the repetition rate at 10 GHz is selected and amplified (microwave generator in figure 1). We note that coherent transfer of spectral properties of an optical oscillator to a microwave could alternatively be designed for optimized robustness, without recurring to a fast optical comb lock [44] as we did. The Cs interrogation signal is synthesized from the 10 GHz input by a two-stage down-conversion. In the first stage, we produce a 9.2 GHz

microwave by mixing to a 800 MHz radio-frequency obtained by downscaling the input 10 GHz signal. This is then brought to resonance with the Cs transition by mixing to a DDS at about 7.4 MHz, adjusted at each clock cycle. The microwave generator noise is dominated by a flicker phase process at the level of -105 dBc Hz^{-1} at 1 Hz, limited by detection and signal conditioning stages, while the flicker phase noise contributed by the synthesis chain is -106 dBc Hz^{-1} at 1 Hz Fourier frequency. The combined effect of the two brings a contributed instability of 5×10^{-16}, with a temperature sensitivity of 0.07 ps K^{-1}. Finally, the ultrastable 1156 nm laser that is used as a seed for the microwave synthesis is measured against IT-Yb1 during the clock operation.

3. Results

3.1. Absolute frequency measurement of Yb

As usual with atomic clocks, data is processed and reported as fractional frequencies $y = r/r_0 - 1$, where r is the frequency measurement and r_0 is an arbitrary reference frequency. For this analysis, the reference is chosen consistent with the recommended value of the secondary representation of the second for the Yb transition, i.e. 518 295 836 590 863.63 Hz, which has an uncertainty of 1.9×10^{-16} as established by CCTF in 2021 [45]. The use of fractional frequency linearizes equations and is convenient for computations with numbers with many digits [16, 46, 47].

We collected data from June 2021 to September 2022. Within this period, we have collected a total of 32 days of data with common uptime between IT-Yb1 and IT-CsF2 using the H-maser chain and a total of 6.9 days of data using the Optical Microwave chain. Data from the combs and IT-Yb1 are collected with a sampling time of 1 s. Data from IT-CsF2, either the frequency measurement relative to the maser or the optically generated microwave, are recorded with a sampling time of 864 s. Data from the optical clock and optical combs are averaged in bins with a duration of 864 s and combined with the Cs fountain data. The recorded data collected in these 864 s bins is shown in figure 2(a), while figure 2(b) shows the same data averaged monthly. The shaded area represents the average fractional frequency ratios over the entire campaign and its uncertainty. All uncertainties include the systematic uncertainties of the clocks.

The instabilities of the comparisons for the entire campaign are shown in figure 3 as overlapping Allan deviations. The comparison through the H-maser chain has an instability at $2.7 \times 10^{-13}/\sqrt{\tau/\mathrm{s}}$ over the full campaign. The comparison through the Optical Microwave chain has slightly lower instability at $2.1 \times 10^{-13}/\sqrt{\tau/\mathrm{s}}$. The improvement is obtained thanks to the lower phase noise of the optically-generated microwave compared to that introduced by the BVA quartz/H-maser system. We have estimated that the contribution of the Dick effect is reduced from $1.6 \times 10^{-13}/\sqrt{\tau/s}$ to a value lower than $3 \times 10^{-15}/\sqrt{\tau/s}$. The best instability observed over a short period of time (less than 1 day) is reduced from $2.1 \times 10^{-13}/\sqrt{\tau/s}$ to $1.3 \times 10^{-13}/\sqrt{\tau/s}$ in high density regime. The residual instability is dominated by the atomic background noise. The average fractional frequency difference between IT-Yb1 and IT-CsF2 is $y(\text{IT-Yb1/IT-CsF2, Optical Microwave chain}) = -3.2(3.7) \times 10^{-16}$ as measured with the Optical Microwave chain and $y(\text{IT-Yb1/IT-CsF2, H-maser chain}) = -3.8(2.9) \times 10^{-16}$ measured with the H-maser chain. The statistical uncertainties are respectively 2.8×10^{-16} and 1.6×10^{-16}, derived from the instabilities shown in figure 3. The weighted average of the two measurements is $y(\text{IT-Yb1/IT-CsF2}) = -3.6(2.7) \times 10^{-16}$, that corresponds to an absolute frequency measurement of $f(\text{IT-Yb1}) = 518\,295\,836\,590\,863.44(14)$ Hz.

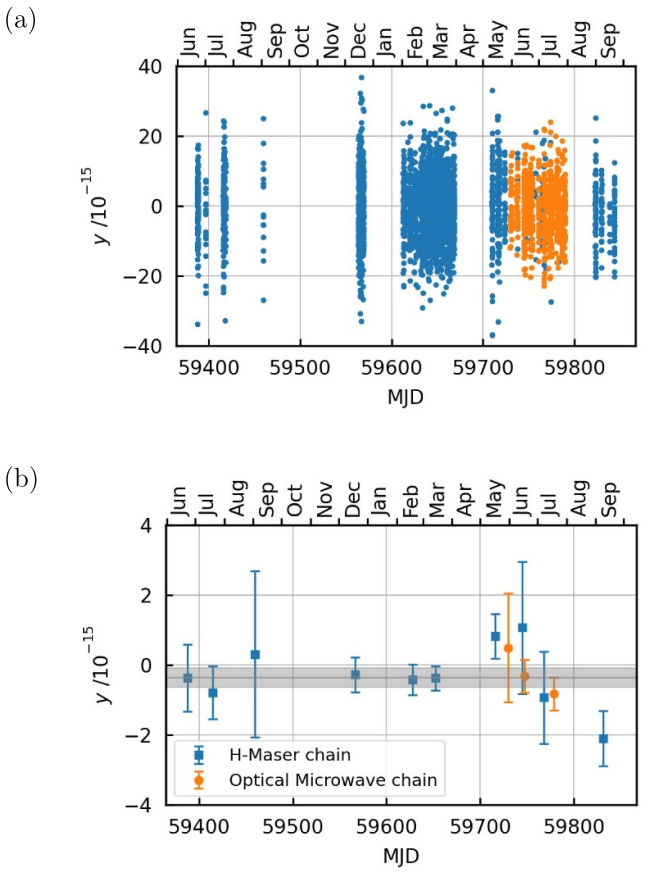

Figure 2. (a) Fractional frequency ratio of IT-Yb1 and IT-CsF2 reported as y (see main text). Data were collected from June 2021 to September 2022 using the H-maser chain (blue dots) and the Optical Microwave chain (orange dots). (b) Same data averaged monthly. The grey line represents the average fractional frequency ratio and the shaded area its uncertainty.

The measurement is limited by the systematic uncertainty of IT-CsF2, including the density shift calculations, that is 2.3×10^{-16} (table 2). The uncertainties of IT-Yb1 (1.9×10^{-17}) and the microwave-to-optical conversion at the combs are negligible. With more than one year of data, the statistical uncertainty limited by the fountain instability is reduced below the systematic contribution. In this way, we avoided the need to increase the fountain measurement time by using the H-maser as flywheel [29, 32, 48], and measurements using the

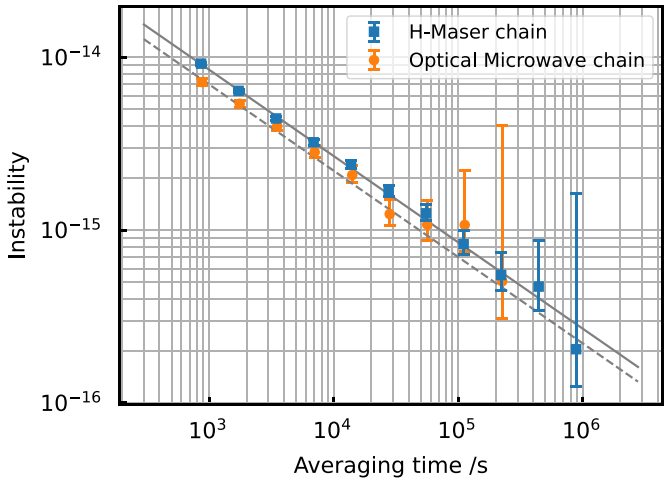

Figure 3. Overlapping Allan deviation of the comparisons over the entire campaign. Orange (blue) dots show data of a measurement carried out using Optical Microwave (H-maser) chain and the dashed (solid) line represents its instability at $2.1 \times 10^{-13}/\sqrt{\tau/\mathrm{s}}$ ($2.7 \times 10^{-13}/\sqrt{\tau/\mathrm{s}}$).

H-maser chain and the Optical Microwave chain are handled in the same way.

3.2. Gravitational coupling of fundamental constants

Clock comparisons have been used to constrain the variations of fundamental constants [49, 50]. For example, violations of the Einstein equivalence principle would result in changes in the frequency ratios of atomic clocks. As a possible application, we investigate the coupling of our frequency measurement to the gravitational potential of the Sun [2, 48, 51–53]. We fit the data in figure 2(a) to $y = y_0 + A\cos(2\pi(t - t_0)/T_0)$, where t is the date of measurement, t_0 is the date of the 2022 perihelion, and $T_0 = 365.26\,\mathrm{d}$ is the duration of the anomalistic year. We find $A = -0.0(2.0) \times 10^{-16}$. The amplitude of the annual variation of the gravitational potential is $\Delta\Phi = 1.65 \times 10^{-10}c^2$, where c is the speed of light. The coupling coefficient of the Yb/Cs ratio to the gravitational potential is then found to be $\beta_{\mathrm{Yb,Cs}} = Ac^2/\Delta\Phi = -0.0(1.2) \times 10^{-6}$. This result shows no violation of the Einstein equivalence principle and has a similar uncertainty while being largely independent to the result in [53]. Following the same approach of [48, 53] it results in a constrain to the gravitational coupling of the electron-to-proton mass ratio of $k_\mu = -0.1(1.2) \times 10^{-6}$. This result can be improved by the continuous long-term operation of frequency standards [2, 50].

4. Conclusions

In this paper, we report the measurement of the clock transition of IT-Yb1 against the primary Cs fountain clock IT-CsF2. The measurement result is $f(\text{IT-Yb1}) = 518\,295\,836\,590\,863.44(14)\,\mathrm{Hz}$ and the total fractional uncertainty, limited by the systematic uncertainty of IT-CsF2, is 2.7×10^{-16}. This is the absolute frequency measurement of Yb against a Cs fountain with the lowest fractional uncertainty. We also show the updated uncertainty budget of IT-Yb1 that has a relative uncertainty of 1.9×10^{-17}. In figure 4 our measurement reported as a red square is compared to the recommended secondary representations of the second and previous absolute frequency measurements [14, 19–29, 54], showing a good agreement. Moreover, we note that this measurement supersedes the local frequency measurement we reported in [19], as it extends the analyzed data period.

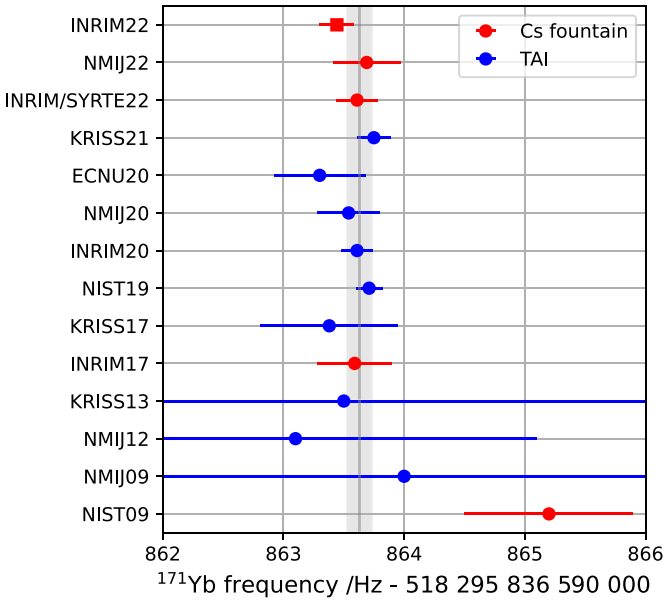

Figure 4. Absolute frequency of Yb performed in several metrological institutes worldwide: red, measurements of Yb against Cs fountains; blue, Yb frequency measurements obtained with a link to TAI. The result of the measurement described in this paper is shown as a red square. The grey solid line and shaded area are respectively the recommended secondary representation of the second and its uncertainty, given by CCTF 2021. All uncertainties correspond to one standard deviation.

These results are a strong demonstration of the improvements achieved in the field of optical clocks and the consequent possibility of introducing a new definition of the second.

Acknowledgments

This work is supported by: the European Metrology Program for Innovation and Research (EMPIR) Projects 18SIB05 ROCIT and 20FUN08 Nextlasers, which have received funding from the EMPIR programme co-financed by the Participating States and from the European Union's Horizon 2020 research and innovation programme.

ORCID iDs

Irene Goti https://orcid.org/0000-0002-4826-6495
Stefano Condio https://orcid.org/0000-0003-4921-7959
Cecilia Clivati https://orcid.org/0000-0002-7289-6403
Matias Risaro https://orcid.org/0000-0001-8046-5710

Michele Gozzelino https://orcid.org/0000-0001-8783-5665
Giovanni A Costanzo https://orcid.org/0000-0002-7474-0349
Filippo Levi https://orcid.org/0000-0002-0206-9082
Davide Calonico https://orcid.org/0000-0002-0345-859X
Marco Pizzocaro https://orcid.org/0000-0003-2353-362X

References

[1] Takamizawa A, Yanagimachi S and Hagimoto K 2022 First uncertainty evaluation of the cesium fountain primary frequency standard NMIJ-F2 *Metrologia* **59** 035004
[2] Guena J *et al* 2012 Progress in atomic fountains at LNE-SYRTE *IEEE Trans. Ultrason. Ferroelectr. Freq. Control* **59** 391–409
[3] Li R, Gibble K and Szymaniec K 2011 Improved accuracy of the NPL-CsF2 primary frequency standard: evaluation of distributed cavity phase and microwave lensing frequency shifts *Metrologia* **48** 283
[4] Beattie S, Jian B, Alcock J, Gertsvolf M, Hendricks R, Szymaniec K and Gibble K 2020 First accuracy evaluation of the NRC-FCs2 primary frequency standard *Metrologia* **57** 035010
[5] Weyers S, Gerginov V, Kazda M, Rahm J, Lipphardt B, Dobrev G and Gibble K 2018 Advances in the accuracy, stability and reliability of the PTB primary fountain clocks *Metrologia* **55** 789–805
[6] Jallageas A, Devenoges L, Petersen M, Morel J, Bernier L G, Schenker D, Thomann P and Südmeyer T 2018 First uncertainty evaluation of the FoCS-2 primary frequency standard *Metrologia* **55** 366
[7] Guéna J *et al* 2017 First international comparison of fountain primary frequency standards via a long distance optical fiber link *Metrologia* **54** 348–54
[8] Blinov I Y, Boiko A I, Domnin Y S, Kostromin V P, Kupalova O V and Kupalov D S 2017 Budget of uncertainties in the cesium frequency frame of fountain type *Meas. Tech.* **60** 30–36
[9] Fang F, Li M, Lin P, Chen W, Liu N, Lin Y, Wang P, Liu K, Suo R and Li T 2015 NIM5 Cs fountain clock and its evaluation *Metrologia* **52** 454–68
[10] Levi F, Calonico D, Calosso C E, Godone A, Micalizio S and Costanzo G A 2014 Accuracy evaluation of ITCsF2: a nitrogen cooled caesium fountain *Metrologia* **51** 270
[11] Guéna J, Abgrall M, Clairon A and Bize S 2014 Contributing to TAI with a secondary representation of the SI second *Metrologia* **51** 108
[12] Beloy K *et al* 2021 Frequency ratio measurements at 18-digit accuracy using an optical clock network *Nature* **591** 564–9
[13] Brewer S M, Chen J-S, Hankin A M, Clements E R, Chou C W, Wineland D J, Hume D B and Leibrandt D R 2019 $^{27}Al^{+}$ quantum-logic clock with a systematic uncertainty below 10^{-18} *Phys. Rev. Lett.* **123** 033201
[14] McGrew W F *et al* 2018 Atomic clock performance enabling geodesy below the centimetre level *Nature* **564** 87–90
[15] Ushijima I, Takamoto M, Das M, Ohkubo T and Katori H 2015 Cryogenic optical lattice clocks *Nat. Photon.* **9** 185–9
[16] Gill P 2016 Is the time right for a redefinition of the second by optical atomic clocks? *J. Phys.: Conf. Ser.* **723** 012053
[17] Lodewyck J 2019 On a definition of the SI second with a set of optical clock transitions *Metrologia* **56** 055009
[18] Riehle F, Gill P, Arias F and Robertsson L 2018 The CIPM list of recommended frequency standard values: guidelines and procedures *Metrologia* **55** 188–200
[19] Clivati C *et al* 2022 Coherent optical-fiber link across Italy and France *Phys. Rev. Appl.* **18** 054009
[20] Lemke N D, Ludlow A D, Barber Z W, Fortier T M, Diddams S A, Jiang Y, Jefferts S R, Heavner T P, Parker T E and Oates C W 2009 Spin-1/2 optical lattice clock *Phys. Rev. Lett.* **103** 063001
[21] Kohno T, Yasuda M, Hosaka K, Inaba H, Nakajima Y and Hong F-L 2009 One-dimensional optical lattice clock with a fermionic ^{171}Yb isotope *Appl. Phys. Express* **2** 072501
[22] Yasuda M *et al* 2012 Improved absolute frequency measurement of the ^{171}Yb optical lattice clock towards a candidate for the redefinition of the second *Appl. Phys. Express* **5** 102401
[23] Park C Y *et al* 2013 Absolute frequency measurement of $^{1}S_0(F = 1/2)$-$^{3}P_0(F = 1/2)$ transition of ^{171}Yb atoms in a one-dimensional optical lattice at KRISS *Metrologia* **50** 119
[24] Kim H, Heo M-S, Lee W-K, Park C Y, Hong H-G, Hwang S-W and Yu D-H 2017 Improved absolute frequency measurement of the ^{171}Yb optical lattice clock at KRISS relative to the SI second *Jpn. J. Appl. Phys.* **56** 050302
[25] Kobayashi T, Akamatsu D, Hosaka K, Hisai Y, Wada M, Inaba H, Suzuyama T, Hong F-L and Yasuda M 2020 Demonstration of the nearly continuous operation of an ^{171}Yb optical lattice clock for half a year *Metrologia* **57** 065021
[26] Luo L *et al* 2020 Absolute frequency measurement of an Yb optical clock at the 10^{-16} level using International Atomic Time *Metrologia* **57** 065017
[27] Kim H, Heo M-S, Park C Y, Yu D-H and Lee W-K 2021 Absolute frequency measurement of the ^{171}Yb optical lattice clock at KRISS using TAI for over a year *Metrologia* **58** 055007
[28] Pizzocaro M, Thoumany P, Rauf B, Bregolin F, Milani G, Clivati C, Costanzo G A, Levi F and Calonico D 2017 Absolute frequency measurement of the $^{1}S_0 \rightarrow {}^{3}P_0$ transition of ^{171}Yb *Metrologia* **54** 102
[29] Pizzocaro M, Bregolin F, Barbieri P, Rauf B, Levi F and Calonico D 2020 Absolute frequency measurement of the $^{1}S_0 \rightarrow {}^{3}P_0$ transition of ^{171}Yb with a link to International Atomic Time *Metrologia* **57** 035007
[30] Grotti J *et al* 2018 Geodesy and metrology with a transportable optical clock *Nat. Phys.* **14** 437–41
[31] Pizzocaro M *et al* 2021 Intercontinental comparison of optical atomic clocks through very long baseline interferometry *Nat. Phys.* **17** 223–7
[32] Nemitz N, Gotoh T, Nakagawa F, Ito H, Hanado Y, Ido T and Hachisu H 2021 Absolute frequency of ^{87}Sr at 1.8×10^{-16} uncertainty by reference to remote primary frequency standards *Metrologia* **58** 025006
[33] Vallet G, Bilicki S, Targat R L and Lodewyck J 2018 Study of accuracy and stability of Sr lattice clocks at LNE-SYRTE *2018 Conf. on Precision Electromagnetic Measurements (CPEM 2018)*
[34] Brown R C *et al* 2017 Hyperpolarizability and operational magic wavelength in an optical lattice clock *Phys. Rev. Lett.* **119** 253001
[35] Beloy K, McGrew W F, Zhang X, Nicolodi D, Fasano R J, Hassan Y S, Brown R C and Ludlow A D 2020 Modeling motional energy spectra and lattice light shifts in optical lattice clocks *Phys. Rev.* A **101** 053416
[36] Nemitz N, Jørgensen A A, Yanagimoto R, Bregolin F and Katori H 2019 Modeling light shifts in optical lattice clocks *Phys. Rev.* A **99** 033424
[37] Lemonde P and Wolf P 2005 Optical lattice clock with atoms confined in a shallow trap *Phys. Rev.* A **72** 033409

[38] Sherman J A, Lemke N D, Hinkley N, Pizzocaro M, Fox R W, Ludlow A D and Oates C W 2012 High-accuracy measurement of atomic polarizability in an optical lattice clock *Phys. Rev. Lett.* **108** 153002
[39] Lodewyck J, Zawada M, Lorini L, Gurov M and Lemonde P 2012 Observation and cancellation of a perturbing dc stark shift in strontium optical lattice clocks *IEEE Trans. Ultrason. Ferroelectr. Freq. Control* **59** 411–5
[40] Lindvall T, Hanhijärvi K J, Fordell T and Wallin A E 2022 High-accuracy determination of Paul-trap stability parameters for electric-quadrupole-shift prediction *J. Appl. Phys.* **132** 124401
[41] Harlander M, Brownnutt M, Hänsel W and Blatt R 2010 Trapped-ion probing of light-induced charging effects on dielectrics *New J. Phys.* **12** 093035
[42] Härter A, Krükow A, Brunner A and Hecker Denschlag J 2014 Long-term drifts of stray electric fields in a Paul trap *Appl. Phys.* B **114** 275–81
[43] Millo J *et al* 2009 Ultralow noise microwave generation with fiber-based optical frequency comb and application to atomic fountain clock *Appl. Phys. Lett.* **94** 141105
[44] Lipphardt B, Gerginov V and Weyers S 2017 Optical stabilization of a microwave oscillator for fountain clock interrogation *IEEE Trans. Ultrason. Ferroelectr. Freq. Control* **64** 761–6
[45] Consultative Committee for Time and Frequency (CCTF) 2021 Recommendation CCTF PSFS 2: updates to the CIPM list of standard frequencies (available at: www.bipm.org/en/committees/cc/cctf/22-_2-2021)
[46] Lodewyck J, Le Targat R, Pottie P-E, Benkler E, Koke S and Kronjäger J 2020 Universal formalism for data sharing and processing in clock comparison networks *Phys. Rev. Res.* **2** 043269
[47] Margolis H S and Gill P 2015 Least-squares analysis of clock frequency comparison data to deduce optimized frequency and frequency ratio values *Metrologia* **52** 628–34
[48] Schwarz R, Dörscher S, Al-Masoudi A, Benkler E, Legero T, Sterr U, Weyers S, Rahm J, Lipphardt B and Lisdat C 2020 Long term measurement of the ^{87}Sr clock frequency at the limit of primary Cs clocks *Phys. Rev. Res.* **2** 033242
[49] Sanner C, Huntemann N, Lange R, Tamm C, Peik E, Safronova M S and Porsev S G 2019 Optical clock comparison for Lorentz symmetry testing *Nature* **567** 204–8
[50] Lange R, Huntemann N, Rahm J M, Sanner C, Shao H, Lipphardt B, Tamm C, Weyers S and Peik E 2021 Improved limits for violations of local position invariance from atomic clock comparisons *Phys. Rev. Lett.* **126** 011102
[51] Dzuba V A and Flambaum V V 2017 Limits on gravitational Einstein equivalence principle violation from monitoring atomic clock frequencies during a year *Phys. Rev.* D **95** 015019
[52] Ashby N, Parker T E and Patla B R 2018 A null test of general relativity based on a long-term comparison of atomic transition frequencies *Nat. Phys.* **14** 822–6
[53] McGrew W F *et al* 2019 Towards the optical second: verifying optical clocks at the SI limit *Optica* **6** 448–54
[54] Kobayashi T *et al* 2022 Search for ultralight dark matter from long-term frequency comparisons of optical and microwave atomic clocks *Phys. Rev. Lett.* **129** 241301